LAWRENCE
LIVERMORE
NATIONAL
LABORATORY

LLNL-PROC-717819

# A Microscopic Theory of Fission

W. Younes, J. A. Brown, E. F. Matthews

January 12, 2017

6th International Conference on "Fission and Properties of Neutron-Rich Nuclei"
Sanibel Island, FL, United States
November 6, 2016 through November 12, 2016

## Disclaimer

# A microscopic theory of fission

W. Younes

*Lawrence Livermore Natl. Lab., Livermore, CA 94551*

J. A. Brown, E. F. Matthews

*Department of Nuclear Engineering, University of California, Berkeley, CA 94720*

We examine the role of non-collective degrees of freedom in fission. we focus in particular on the use of the quasiparticle random-phase approximation (QRPA) to study the population mechanisms of the fissioning nucleus, and the Schrödinger collective intrinsic model (SCIM) to allow for quasiparticle excitations during fission. The QRPA calculations are performed with the D1S finite-range effective interaction for $^{240}$Pu while the SCIM is applied to a level-density calculation for the schematic multi-$O\,(4)$ model.

## 1. Introduction

One the interesting aspects of fission theory concerns the role played by single-particle degrees of freedom. Fission is understood to be a primarily collective phenomenon, but non-collective (single-particle) states are expected to play an important role both in the initial excitation mechanism of the fissioning nucleus[1] and throughout its subsequent evolution to scission[3,4]. In this paper we explore two formalisms that can be used to include non-collective modes in the theoretical description of fission: the quasiparticle random phase approximation (QRPA) and the Schrödinger collective-intrinsic model (SCIM). This work builds on earlier studies performed using the generator-coordinate method within the Gaussian-overlap approximation (GCM+GOA)[5]. In order to provide a context for the new results presented here, we first recall the earlier GCM+GOA work.

A comprehensive review of microscopic approaches to fission in general, and with the GCM+GOA in particular, can be found in the recent publication by Schunck and Robledo[6]. Starting from constrained Hartree-Fock-Bogoliubov (HFB) calculations, performed in this case with the D1S effective interaction[7], the GCM constructs a nuclear wave function as a linear superposition of the HFB solutions that can be static,

$|\Psi\rangle = \int dq\, f(q)\, |\Phi(q)\rangle$, or time-dependent, $|\Psi(t)\rangle = \int dq\, f(q,t)\, |\Phi(q)\rangle$, where $|\Phi(q)\rangle$ is the HFB state calculated with a constraint (or with multiple constraints) value(s) $q$. The unknown coefficients $f(q)$ or $f(q,t)$ then have to be determined. A variational principle with respect to these unknown coefficients is applied to the energy $E = \langle\Psi|H|\Psi\rangle$ (or to $\langle\Psi(t)|H - \hbar i\partial/\partial t|\Psi(t)\rangle$ in the time-dependent case), where $H$ is the HFB Hamiltonian. This produces the well-known Hill-Wheeler equation [8]. In practice, this integro-differential equation is very difficult to solve with more than one constraint [9,10]. Therefore, in previous work we adopted a standard set of approximations by assuming a Gaussian form for the overlap of HFB states, $\langle\Phi(q)|\Phi(q')\rangle$, and expanding the Hamiltonian overlaps $\langle\Phi(q)|H|\Phi(q')\rangle$ to $2^{\text{nd}}$ order in $q - q'$. The result is a Schrödinger-like equation in the collective parameter(s) $q$ where the collective Hamiltonian is constructed from the underlying single-particle degrees of freedom [7,11]. Thus the inertia tensor, the potential energy, and the zero-point energy (ZPE) correction are all calculated from the HFB wave functions. The static collective Schrödinger equation produces a spectrum of initial fissioning states, and the time-dependent equation evolves those initial states to a set of scission configurations (scission line) where we extract fission-fragment properties such as their mass distributions, total kinetic energies (TKE's), and total excitation energies (TXE's).

The calculations presented in Younes et al. [5] differed from previous work [7,11] in several respects. First, instead of the usual quadrupole ($Q_{20}$) and octupole ($Q_{30}$) moments, the separation distance and mass difference between pre-fragments were used as constraints in the HFB calculations in order to avoid a persistent problem with missing yield for certain mass ranges in the fragment distribution [12]. Second, quantum localization was used [13] to: 1) progressively recognize the wave functions of the pre-fragments within the wave function of the parent nucleus, 2) impose a quantum-mechanical criterion for scission, and 3) calculate the static contributions to the TKE and TXE at scission. Finally, the dynamical contribution to the TKE and TXE (i.e., the pre-scission energies) were estimated from an analysis of the flux in the fission direction and by using the WKB approximation to relate that flux to energy [5]. In this previous work we calculated the fragment mass distribution for the $^{239}\text{Pu}\,(n,f)$ reaction from thermal to 5-MeV incident neutron energies. These mass distributions were found to agree with data at thermal energies, and with a phenomenological model at higher energies, where data are not available. We also calculated the TKE and TXE for $^{239}\text{Pu}\,(n_{th},f)$ and compared them to

data. Although the agreement between theory and experiment was good, the TKE were systematically overestimated by the theory, while the TXE were underestimated. These deviations could be caused by missing degrees of freedom, and in particular by quasiparticle states excited during the fission process that would increase the TXE while reducing the TKE.

## 2. QRPA calculations for $^{240}$Pu

The work presented here is strongly inspired by that of Péru and Martini [1] but also many others, especially in the context of the finite-amplitude method (FAM) [14–17]. Unlike the GCM+GOA approach described in the previous section, the QRPA is not limited to motion described by a few collective parameters, and can be used to describe both collective and non-collective quasiparticle (qp) excitations. Its main limitation is that it assumes harmonic motion. The QRPA is derived in many references [1,18].

For the present work, a code was written to solve the full QRPA matrix equation and applied to $^{240}$Pu using the D1S finite-range interaction in a deformed harmonic-oscillator basis [19] to generate excitations of the system. Optimization was a crucial focus in the code development since QRPA calculations can rapidly become unwieldy as the size of the configuration space (i.e., the number of qp states) increases. The performance of the code was improved by exploiting both data parallelism and the systematic pre-calculation of often-used quantities identified through benchmarking.

The solutions to the QRPA equation were used to calculate a photoabsorption cross section on the $^{240}$Pu ground state using the formalism in Oishi et al. [17] with a Lorentzian smearing width $\Gamma = 1$ MeV. Despite the code optimizations mentioned above however, additional restrictions had to be imposed to accommodate the available computational resources. Thus only shells $N_{\rm sh} = 0-10$ of the harmonic-oscillator basis were used, and only 2-qp excitations below 80 MeV were included. The resulting cross section is shown in Fig. 1, where it is compared to the ENDF/B-VII.1 evaluation, obtained with a Hauser-Feshbach calculation. While the QRPA results appear to be converged as function of the 2-qp cutoff energy, the cutoff at $N_{\rm sh} = 10$ is probably not adequate. Calculations that include up to the $N_{\rm sh} = 12$ shell would be more appropriate [1]. The FAM [14–17] should provide a more efficient alternative in this case.

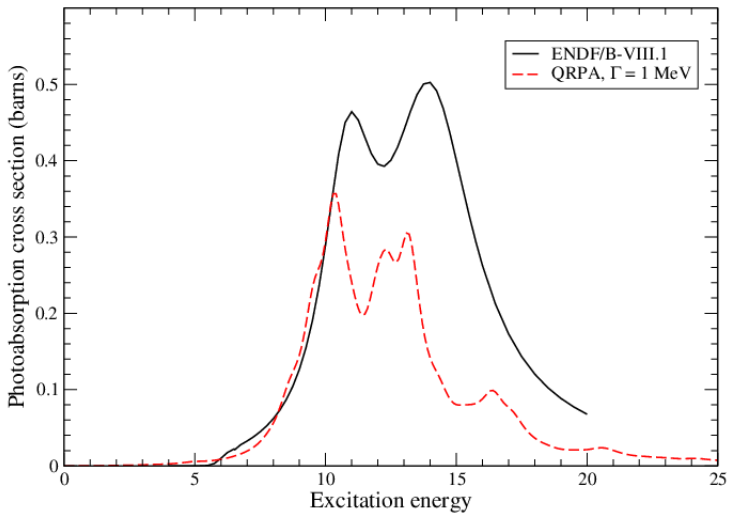


Figure 1. Photoabsorption cross section on the $^{240}$Pu ground state calculated using the QRPA and compared to the ENDF/B-VII.1 evaluation.

## 3. Exploring the SCIM with a schematic model

The SCIM was developed as part of the Ph.D. thesis of R. Bernard[2]. The model follows pioneering work from the 1970's onward seeking to include qp excitations within the GCM framework[20,21]. In the SCIM, the usual GCM ansatz in section 1 is extended to include 2-qp excitations, $|\Psi\rangle = \int dq\, f_0(q)\, |\Phi_0(q)\rangle + \sum_{i>0} \int dq\, f_i(q)\, |\Phi_i(q)\rangle$, where the index $i = 0$ refers to the HFB ground state, and $i > 0$ labels 2-qp excitations built on that ground state. A time-dependent version can also be introduced if needed. The variational principle with respect to the weight functions $f_i(q)$ (where $i = 0, 1, \ldots$) then leads to a Hill-Wheeler equation where the overlaps $H_{ij}(q, q') \equiv \langle \Phi_i(q) | H | \Phi_j(q') \rangle$ and $N_{ij}(q, q') \equiv \langle \Phi_i(q) | \Phi_j(q') \rangle$ are matrices. The same effective interaction that describes the HFB ground state also gives the coupling between ground state and 2-qp excitations and among 2-qp states. The full derivation of the SCIM can be found in

Bernard et al.[2] and produces a Schrödinger-like equation with Hamiltonian

$$\mathscr{H} = \sum_j \left\{ \frac{1}{2} \left[ \left[ M^{-1}(q) \right]_{ij} \hat{P} \right]^{(2)} + \left[ T_{ij}(q) \hat{P} \right]^{(1)} + V_{ij}(q) \right\} \tag{1}$$

where $\hat{P} \equiv i\partial/\partial q$, and where we have introduced the symmetric ordered products of operators (SOPO's) defined for an arbitrary operator $A$ as $\left[ A^{(n)}(q) \hat{P} \right]^{(n)} \equiv \frac{1}{2^n} \sum_k \binom{n}{k} \hat{P}^{n-k} A^{(n)}(q) \hat{P}^{(k)}$ and which depend on the symmetrized moment $A^{(n)}(q) \equiv i^n \int_{-\infty}^{+\infty} ds\, s^n \left\langle \Phi_i \left( q + \frac{s}{2} \right) |A| \Phi_j \left( q - \frac{s}{2} \right) \right\rangle$. In Eq. (1) the matrices $M(q)$, $T(q)$, and $V(q)$ can be expressed in terms of the symmetrized moments $H^{(n)}$ and $N^{(n)}$ and their derivatives with respect to $q$. The SCIM formalism thus eliminates the GOA, which implicitly assumes collective modes[22], and can therefore be used to describe non-adiabatic phenomena (e.g., the excitation of qp states during fission).

The eventual goal is to apply the SCIM to the fission problem with multiple constraints and all relevant 2-qp excitations. This program represents a natural extension to the work presented in section 1. As a more tractable step in that direction, we present calculations using a schematic model of the nucleus: the multi-$O(4)$ model[23,24]. This model can be thought of as a simplified version of the pairing+quadrupole model (with only $K = 0$ terms), and for our purposes we will limit it to only one type of nucleon. We consider a "nucleus" consisting of $N$ identical particles in $n$ shells labeled by half-integer spin $j$, and where each shell consists of degenerate states of common energy $e_j^0$ and "deformation" $d_j$, labeled by the quantum number $m = -j, -j-1, \ldots, j-1, j$. Each $m$ state can hold 2 nucleons so that a $j$ shell contains at most $\Omega_j = j + 1/2$ pairs of particles. The Hamiltonian of the system is

$$\hat{H} = \sum_j e_j^0 \hat{N}_j - \frac{1}{2} \chi \hat{D}^2 - \frac{1}{2} G \left( \hat{A}^\dagger \hat{A} + \hat{A} \hat{A}^\dagger \right) \tag{2}$$

where we have defined a number operator $\hat{N}_j \equiv \sum_m a_{jm}^\dagger a_{jm}$ for each shell $j$ in terms of the particle creation and annihilation operators $a_{jm}^\dagger$ and $a_{jm}$, a "deformation" operator $\hat{D} \equiv \sum_j d_j \sum_m \sigma_{jm} a_{jm}^\dagger a_{jm}$ with $\sigma_{jm} = +1$ if $|m| < \Omega_j/2$ and -1 if $|m| > \Omega_j/2$, and an operator $\hat{A}^\dagger \equiv \sum_j \sum_{m>0} a_{jm}^\dagger a_{j\bar{m}}^\dagger$ with $\bar{m}$ designating the time-reversed state. Matrix elements of the Hamiltonian in Eq. (2) between many-body states can be calculated exactly using quasi-spin methods[23,24]. This makes the multi-$O(4)$ model particularly attractive as a test bed for the SCIM. A numerical diagonalization of Eq. (1)

with the Hamiltonian in Eq. (2) was obtained for a system of 28 particles, 3 shells with $j = 27/2, 19/2, 7/2$, $e_j^0 = 0.0, 1.0, 3.5$, $\chi = 0.04$, and $G = 0.14$ in dimensionless "energy" units[23,24]. To do this, the deformation parameter $\left\langle \hat{D} \right\rangle$ was discretized and Eq. (1) was turned into a matrix diagonalization problem. The convergence of the eigenvalues with respect to the step size in $\left\langle \hat{D} \right\rangle$ was verified. In addition a study of the behavior of these eigenvalues as a function of the coupling between states was performed. This was accomplished by introducing a parameter $\kappa$ multiplying the matrix elements connecting the ground state to 2-qp states, or connecting 2-qp states to one another. For $\kappa = 0$ many solutions were found with zero eigenvalue and zero eigenvector component in the ground state. These pure 2-qp excitations are not physical solutions in the $\kappa = 0$ case, which should consist entirely of superpositions of HFB ground states from the different $\left\langle \hat{D} \right\rangle$ values. Therefore, they were treated as spurious states. Furthermore, as $\kappa$ increases from 0 to 1, many of the spurious solutions with 0 component in the ground states persist and "pollute" the entire energy spectrum. These spurious solutions have also been ignored.

In Fig. 2 we have plotted the cumulative number of levels as a function of excitation energy for the numerical example above. The figure shows the results of calculations obtained from 1) the exact solution of the multi-$O\,(4)$ model, 2) the GCM with particle-number projection, and 3) the SCIM solution using the approach described above. Below an excitation energy of 9, both the GCM and SCIM solutions give comparable results that underestimate the cumulative level count for the exact solution by roughly similar amounts. For energies above 9, the GCM starts to run out of levels and approaches a plateau, whereas the SCIM curve continues to rise with a slope that is similar to the exact solution's.

## 4. Conclusion

The QRPA was used with a finite-range interaction to calculate the photoabsorption cross section for $^{240}$Pu, and the results were compared to a standard Hauser-Feshbach calculation. In the future, limitations in the basis size and configuration space could be overcome through the use of the finite-amplitude method. Next, the SCIM was investigated using the schematic multi-$O\,(4)$ model. The cumulative level density obtained using the SCIM was compared to an exact solution of the multi-$O\,(4)$ model. Several improvements to the SCIM calculation will be investigated in future work: the effect of particle-number projection, the use of local QRPA exci-

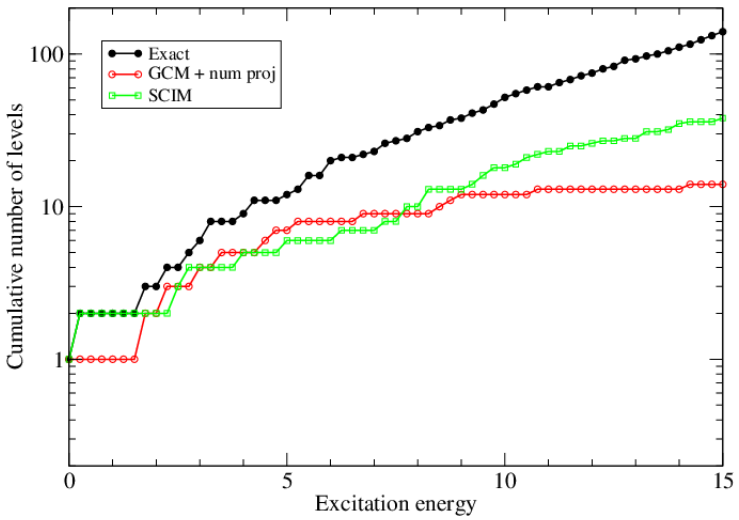


Figure 2. Cumulative level density for the multi-$O(4)$ model example (see text) as a function of (unitless) excitation energy. Calculations from the exact solution, the GCM with particle-number projection, and the SCIM are compared.

tations at each deformation instead of uncorrelated 2-qp states (the QRPA solutions would provide 2-qp excitations that are orthogonal to the local ground state to better separate vibrations in $\left\langle \hat{D} \right\rangle$ from other modes), and extensions to 4-qp excitations and terms beyond $2^{\text{nd}}$-order SOPO's.

## 5. Acknowledgments

This work was performed under the auspices of the U.S. Department of Energy by Lawrence Livermore National Security, LLC, Lawrence Livermore National Laboratory under Contract DE-AC52-07NA27344. This material is based upon work supported by the Department of Energy National Nuclear Security Administration under Award Numbers DE-NA0003180 and DE-NA0000979.

## Bibliography

1. S. Péru and M. Martini, Eur. Phys. J. A 50, 88 (2014).

2. R. Bernard, H. Goutte, D. Gogny, and W. Younes, Phys. Rev. C 84, 044308 (2011).
3. J. R. Nix, A. J. Sierk, H. Hofmann, F. Scheuter, and D. Vautherin, Nucl. Phys. **A424**, 239 (1984).
4. N. Carjan, P. Talou, O. Serot, Nucl. Phys. A792, 102 (2007).
5. W. Younes, D. Gogny, and N. Schunck, Proc. of the Fifth International Conference on ICFN5, Sanibel Island, Florida, USA, 4-10 Nov. 2012, p. 605, World Scientific, Eds. JH Hamilton and AV Ramayya (2013).
6. N. Schunck and L. M . Robledo, Rep. Prog. Phys. 79, 116301 (2016).
7. J.-F. Berger, M. Girod, and D. Gogny, Comp. Phys. Comm. 63, 365 (1991).
8. D. L. Hill and J. A. Wheeler, Phys. Rev. 89, 1102 (1953).
9. P. Bonche, J. Dobaczewski, H. Flocard, P.-H. Heenen, J. Meyer, Nucl. Phys. **A510**, 466 (1990).
10. L. M. Robledo, G. F. Bertsch, Phys. Rev. C 84, 054302 (2011).
11. H. Goutte, J. F. Berger, P. Casoli, and D. Gogny, Phys. Rev. **C 71**, 024316 (2005).
12. N. Dubray and D. Regnier, Comp. Phys. Comm. 183, 2035 (2012).
13. W. Younes and D. Gogny, Phys. Rev. Lett. 107, 132501 (2011).
14. P. Avogadro and T. Nakatsukasa, Phys. Rev. C 87, 014331 (2013).
15. N. Hinohara, M. Kortelain, and W. Nazarewicz, Phys. Rev. C 87, 064309 (2013).
16. T. Nikšić, N. Kralj, T. Tutiš, D. Vretenar, and P. Ring, Phys. Rev. C 88, 044327 (2013).
17. T. Oishi, M. Kortelain, and N. Hinohara, Phys. Rev. C 93, 034329 (2016).
18. P. Ring, P. Schuck, *The Nuclear Many-Body Problem* (Springer, Heidelberg 1980).
19. W. Younes, Comp. Phys. Comm. 180, 1013 (2009).
20. M. Didong, H. Müther, K. Goeke, A Faessler, Phys. Rev. C 14, 1189 (1973).
21. N. Tajima, H. Flocard, P. Bonche, J. Dobaczewski, P.-H. Heenen, Nucl. Phys. A551, 409 (1993).
22. P. G. Reinhard and K. Goeke, Rep. Prog. Phys. 50, 1 (1987).
23. M. Kobayasi, T. Nakatsukasa, M. Matsuo, K. Matsuyanagi, Prog. Theor. Phys. 110, 65 (2003).
24. N. Hinohara, T. Nakatsuakasa, M. Matsuo, K. Matsuyanagi, Prog. Theor. Phys. 115, 567 (2006).